Quantitative assessment of individual populations present in nanoparticle – antibody conjugate mixtures using AF4 – ICP-MS/MS

Diego Bouzas-Ramos, Jose Ignacio García Alonso, Jose Manuel Costa-Fernández* and Jorge Ruiz Encinar*

Department of Physical and Analytical Chemistry, University of Oviedo, Avda. Julián Clavería 8, 33006, Oviedo, Spain

ABSTRACT

A remaining challenge nowadays in nanotechnology is the fast and reliable determination of the ratios between engineered nanoparticles and the species attached to their surface after chemical functionalization. The approach proposed herein based on the on-line coupling of asymmetric flow field-flow fractionation (AF4) with inductively coupled plasma-tandem mass spectrometry (ICP-MS/MS) allows for the first time the direct determination of such ratios in CdSe/ZnS core-shell Quantum Dot : rat monoclonal IgG2a antibody (QD:Ab) conjugate mixtures in a single run without any previous sample preparation (i.e. derivatization). AF4 provides full recovery and adequate resolution of the resulting bioconjugate from the excess of nanoparticles and proteins used in the different bioconjugation mixtures (1:1, 2:1 and 3:1, QD:Ab molar ratios were assessed). The point-by-point determination by ICP-MS/MS of the metal to sulfur ratios along the bioconjugate fractographic peak allowed disclosing the mixture of the different species in the bioconjugated sample, providing not only the limits of the range of QD:Ab ratios in the different bioconjugate species resulting after functionalization but a good estimation of their individual relative abundance in the mixture as well. Interestingly, a wide variety of compositions were observed for the different bioconjugate mixtures studied (QD:Ab molar ratios ranging from 0.27 to 4.6). The resulting weighted QD:Ab ratio computed in this way for each bioconjugate peak matches well with both the global (average) QD:Ab ratio experimentally obtained by the simpler peak area ratio computation and the theoretical QD:Ab molar ratios assayed, which internally validates the procedure developed.

Since the development of first strategies for controlled synthesis of inorganic nanoparticles (NPs), especially Quantum Dots (QDs), a myriad of procedures have been carried out for their functionalization with appropriate biomolecules (*e.g.* antibodies, aptamers, etc.) to ensure their specific interaction with target molecules and analytes for *in vitro* and *in vivo* bioanalytical applications.[1,2] In fact, control of the functionalization of the NPs surface with different ligands and biomolecules is key to ensure success of their application. Unfortunately, there is not yet a standard method available to determine the ratio between NPs and the biomolecules functionalized to their surface after the corresponding bioconjugation reaction. There is therefore an urgent need for novel and reliable quantitative methods to face this challenge.[3,4]

In this context, spectroscopic techniques, such as fluorescence or UV-visible spectroscopy, can give an estimation of the amount of molecules attached onto NPs surface via free protein quantification in the supernatant of the reaction.[5,6] Such indirect analysis only provides average NP:biomolecule ratio in the final solution without any information about the interaction between them. In contrast, gel electrophoresis is able to separate discrete NP-biomolecule conjugates.[7] However, quantification after the gel separation is difficult and is commonly carried out off-line by removing and extracting the desired bands prior to the analysis (*e.g.* by immunoassay measurements, etc.).[8] Moreover, this technique is limited by the complex interaction of the different NPs and their surface functional groups with the gel sieving and the separation capacity as well. Finally, not all NP-biomolecule conjugates are amenable to be separated using this strategy.[9] Recently, accurate determination of protein coverage over NP surface has been achieved by quantification of the total protein bound.[10] However, it requires complex sample treatment, including protein digestion followed by HPLC-fluorescent analysis of the resulting amino acids after derivatization. Unfortunately, this last approach does not provide any information about the dispersion of the different NP:protein populations present.

Determination of metal to sulfur ratios by inductively coupled plasma-mass spectrometry (ICP-MS) appears to be a promising alternative to estimate the NP:biomolecule ratio in nanoassemblies, as different ICP-detectable elements are present in most inorganic NPs and biomolecules (*e.g.* sulfur in proteins). For instance, determination of bulk metal to sulfur ratios has been already reported for the quantification of the ligand density on the surface of NPs[11-13] and the average protein corona content in gold NPs.[14,15] Moreover, very often, S is present not only in the biomolecule but also in the core or shell of the NPs (e.g. ZnS, AgS, CdS),[16] thereby

making the use of ICP-MS more difficult. The introduction of enriched ^{34}S isotope in the engineered nanoparticle structure followed by a single mass spectrometric sulfur isotope ratio measurement allowed the assessment of nanoparticle-biomolecule stoichiometries.[17] Of course, this procedure requires a previous synthesis of the nanoparticles incorporating the enriched S. Unfortunately, all the ICP-MS-based strategies so far, although very useful for studying interactions between NPs with S-containing biomolecules, provide exclusively the average ratio of the molecules (*e.g.* ligands, proteins, etc.) attached to the NP.

Herein, we propose a new and simple approach that allows direct assessment of the various conjugate populations with different ratios QDs to antibody (Ab) present in bioconjugate mixtures. First, direct injection of the resulting bioconjugate mixture into the AF4–ICP-MS/MS system would provide full recovery and complete isolation of the target broad bioconjugate peak from the corresponding excesses of QDs and Ab used during the bioconjugation reaction. Second, simple determination by ICP-MS/MS of the metal to sulfur ratios along the bioconjugate peak obtained would allow not only to compute the global (average) QD:Ab ratio but disclosing the mixture of the different species with different QD:Ab ratios eventually present in the bioconjugated sample with an estimation of their relative abundance.

EXPERIMENTAL SECTION

Instrumentation

UV-vis absorbance was recorded on a Genesys 10S Spectrophotometer (Thermo Scientific, Germany). Fluorescence emission was measured using a Varian Cary Eclipse (Agilent, Germany) fluorescence spectrophotometer (excitation wavelength 350 nm, excitation and emission slits width 5 nm). Conventional Quartz SUPRASIL cuvettes (Hellma Analytics, Germany) were used.

The AF4 system used was an AF2000 (Postnova Analytics, Germany). Regenerated cellulose membrane with 10 kDa cut-off was used as accumulation wall. Table S1 summarizes the channel characteristics and the flow rate program employed. After completion of the elution program, cross flow rate was maintained at 0.0 mL min^{-1} (10 min) to ensure complete elution of all species. The AF4 effluent was coupled on-line to an ICP-MS/MS (Agilent 8800, Japan) to obtain a virtually interference-free and sensitive detection of S.[18,19] Oxygen was introduced in the

reaction cell at a flow of 0.35 mL min^{-1}. S and Se were detected in mass shift MS/MS mode (^{32}S$^+$→^{48}SO$^+$ and ^{80}Se$^+$→^{96}SeO$^+$, respectively) whilst Cd was measured in on mass mode (^{106}Cd$^+$→^{106}Cd$^+$). Integration time was 0.1 s. Operation conditions were daily optimized and are summarized in Table S2. Integration of the fractographic peaks was performed using the *MassHunter* software (Agilent).

Synthesis, water-stabilization and conjugation of the CdSe/ZnS QDs with Antibodies

CdSe/ZnS core-shell QDs were synthesized in our laboratory using the organometallic route described by Peng *et al.*[20] (see Supporting Information). Resulting non-polar QDs suspended in chloroform were then transferred to aqueous media using an amphiphilic polymer.[21,22] The obtained polymer-coated QDs were dispersed in a 50 mM borate buffered saline solution (SBB) at pH 12 and subjected to ultrafiltration (5 cycles at 5000 rpm during 5 min) using 100 kDa cut-off membrane filters to remove the possible excess of reagents.

CdSe/ZnS QDs were conjugated to standard Ab (rat monoclonal IgG2a, Acris Antibodies, Herford, Germany) through the modification of the carboxyl groups of the outer polymeric layer of the water-stabilized QDs by *EDC chemistry* for the subsequent attachment of the amine groups of the Ab.[23] The QD:Ab mixtures assayed in this study ranged from equimolar molar ratio (1:1) to excess of QDs per Ab (2:1 and 3:1). Molar concentration of the Ab used was kept constant (0.5 μM). EDC and NHS were used in a molar excess of 1500.

RESULTS AND DISCUSSION

Two independent strategies have been developed to quantitatively assess bioconjugation between engineered CdSe/ZnS QDs synthesized in our laboratory and a standard monoclonal antibody with a known amino acid sequence. First one, schematically illustrated in Figure 1, provides the global (average) QD:Ab ratio in the different bioconjugated mixtures resulting after the chemical reaction. Briefly, it relies on the measurement of Cd to S area ratios in the AF4 peaks obtained for pure and isolated bioconjugated QDs, which are then translated into the corresponding Cd to S molar ratios using external Flow Injection (FI) calibration. As the number of S atoms per mol of antibody is known beforehand and the number of Cd and S atoms per QD could be obtained,

we can then easily translate the Cd to S molar ratio determined in the bioconjugate peak into the sought global (average) QD to antibody ratio.

Second strategy, illustrated in Figure 2, allows disclosing the mixture of the different species with different QD:Ab ratios eventually present in the bioconjugated sample. Briefly, it relies on the point-by point determination of the Cd to S intensity ratio along the bioconjugate peak obtained, which changes significantly along its central part because of the continuous elution of unresolved bioconjugated species with increasing QD:Ab ratios. In contrast, two regions with stable Cd to S ratios are observed at the beginning and end of the bioconjugate peak that can be ascribed to the parts of the limit populations with lowest and highest QD:Ab ratios eluting lonely from the AF4. Intensity ratios for the pure QD and the two limit bioconjugate populations are translated into Cd to S molar ratios using again external FI calibration. Such molar ratios, together with the number of S atoms in the antibody and the number of Cd and S atoms per QD, can be used to obtain the individual QD:Ab ratios for the lower and upper limit populations. The mathematical treatment developed herein, and schematized in Figure 3, can be then used to estimate their individual relative abundances within the bioconjugate mixture.

It is clear then that characterization of the pure QDs and complete separation of the bioconjugate mixture from the corresponding QD, antibody and free-metal excesses are required and thus will be briefly explained before the detailed description of the 2 strategies developed.

Characterization of the CdSe/ZnS QDs Used

Synthesized water-stable CdSe/ZnS QDs showed an intense sharp fluorescence emission at 605 nm with a full width at half maximum of the emission band of 40 nm, indicating low nanoparticle size dispersion (see Figure S1). UV-vis was used to estimate[24] that the NP core size was 3.8 ± 0.4 nm and the QD concentration in the stock solution was 2.9 ± 0.2 μM.

Number of Cd atoms present per QDs was determined as well by direct ICP-MS/MS analysis of the acid digested QDs solution. Both Cd and QDs concentrations and corresponding uncertainties were then related and the resulting Cd atoms per QD obtained was 205 ± 14 (1SD, *n*=3). On the other hand, Cd/S peak area ratio of the pure QDs (see Figure 1) experimentally obtained by AF4-ICP-MS/MS could be translated into the corresponding Cd/S molar ratio using an external calibration curve built using inorganic ICP standards of each element and Flow Injection Analysis (see Figures S2a and S2b). Finally, taking into account the number of Cd

atoms per QDs and the Cd/S molar ratio value determined for the pure QDs (see Figure 1), a value of 95 ± 7 S atoms per QDs (1SD, n=3) was obtained. It is important to note that such indirect determination of the S atoms per QDs was carried out in order to minimize any error that could likely occur due to S contamination coming from the reagents used during the QDs digestion as well as eventual S losses.

Separation of Nanoparticulated Species and Bioconjugation Efficiency Determination

We have already demonstrated that using AF4 under optimized conditions[23] (summarized in Table S1), we are able to clearly separate the excesses of free antibodies and free QDs, which coelute at 10 min (see fractograms for pure Ab and QDs in Figures S3a and S3b, respectively) from the bioconjugate peak, which elutes at ~14 min (see Figures S3c-e). Remarkably, quantitative AF4 recovery (95 ± 3 %, 1SD, n=3) obtained for the bioconjugate mixture demonstrated that all nanoparticulated species were recovered completely from the AF4 system. Different bioconjugation mixtures, with 1:1, 2:1 and 3:1, QD:Ab molar ratios, were assessed (see Figures S3c-e). The reason behind of evaluating these ratios is the subsequent application of these nanoassemblies in immunoanalysis. Bioconjugation of several QDs to a specific antibody would enable to enhance the sensitivity of either ICP-MS or fluorescence detection of targeted biomarkers in immunoassays. It should be borne in mind, however, that bioconjugation of too many QDs would bring about that recognition capabilities of the antibody could be hindered, which adversely affect the corresponding immunoassay.[25] Comparison of the Cd area for the peaks corresponding to QD excess and bioconjugate provides directly the efficiency of the bioconjugation reaction under the different conditions assayed. As it can be clearly seen in Table 1, it increases under excess of QDs per antibody from 60 ± 2 % to 74 ± 2 % (n=3). These expected results are in agreement with those obtained previously.[23]

Strategy 1: Determination of the Global (average) QD:Ab Ratio

We first measured Cd/Se and Cd/S elemental area ratios in order to confirm the nature of the bioconjugate peak after AF4 separation. Results are collected in Table 1. Precision was adequate ranging from 1 to 4 % RSD. As expected, Cd/Se area ratios observed in the bioconjugation peak for the different mixtures assayed were very consistent between them and with the one obtained for the pure QDs (1.79 ± 0.04; 1SD, n=3) as the core/shell of the QDs does not change after the

bioconjugation reaction and the bioconjugated Ab contains neither Cd nor Se. For the same reason, Cd/Se area ratios obtained in the fractographic peaks where QDs and Ab excesses elute for the different mixtures assayed were also similar (1.73 ± 0.05; 1SD, n=3). In contrast, as can be seen in Table 1, Cd/S area ratios obtained for the bioconjugate peak were significantly different than that observed for the pure QDs (1.85 ± 0.05; 1SD, n=3). Additionally, the magnitude of this difference decreases as the QD:Ab ratio assayed increases. This finding is again expected because the bioconjugation reaction of an Ab to the QDs brings new S atoms (present in the amino acid sequence of the Ab) into the bioconjugate species and, thus, lowers the Cd/S ratio in the bioconjugate peak, confirming that the second fractographic peak for the different mixtures assayed (Figures S3c-e) corresponds to the QD-Ab bioconjugate. Of course, the higher the ratio QD:Ab in the bioconjugate, the closer its Cd/S ratio to the pure QD since the impact of the S coming from the antibody is reduced. It is worth stressing that we used the Cd/S molar ratio obtained for the pure QDs as reference value since the Cd/S molar ratios obtained for those fractographic peaks where QDs excess elutes (peak at 10 min in Figures S3c-e) varied significantly for each bioconjugation reaction assayed (1.57 ± 0.08, 1.96 ± 0.07, 1.95 ± 0.07, respectively; 1SD, n=3). This is expected as the excess of Ab coelutes at 10 min shifting the Cd/S molar ratio for each reaction mixture depending on the corresponding amounts of QDs and Abs in excess.

Scheme of the workflow employed for the determination of the global ratio QD to Ab in the bioconjugates is given in Figure 1. Since elemental Cd and S signals provided by the ICP-MS/MS are virtually species-independent, quantitative and accurate determination of the QD:Ab molar ratios in the different bioconjugates peaks could be achieved for the first time. Such challenging and interestingly parameter could be obtained by resorting to external FI calibration, where different mixtures of Cd and S standards were analyzed to build a curve where Cd/S area ratios were plotted against corresponding Cd/S molar ratios (see Figure S2). Since number of Cd and S atoms present per QD was previously determined accurately and number of S atoms per Ab molecule is known (54 S atoms/Ab), we were able to clearly distinguish the S contribution coming from the Ab and the QDs in each bioconjugate peak. Taking all these data together with the Cd/S molar ratio computed for each bioconjugate peak using the FI calibration curve, we could afford determination of the global QD:Ab ratio for each bioconjugate mixture. It is important to note that uncertainty was propagated taking into account each experimental

parameter used in the corresponding QD:Ab ratio computation and finally ranged from 8 to 10% RSD (n=3). As can be seen in Table 1, experimental results obtained fit pretty well with the theoretical QD:Ab ratios assayed for the different bioconjugates.

Strategy 2: Determination of QD:Ab Ratios of Individual Limit Populations and their relative abundance

We have demonstrated that isolation of free QDs and Ab from the bioconjugate peak allowed the computation of the average QD:Ab ratio of the bioconjugate mixture using the Cd/S area ratio. However, such bioconjugate peak is likely constituted by a collection of individual bioconjugated species with different QD-Ab ratios and relative abundances. In fact, as it can be observed in the fractograms shown in insets of Figure 1 and 2 and Figures S3c-e, bioconjugate peak (~14 min) is significantly broader than the peak corresponding to the excess of free QDs (~10 min), which seems to indicate the coelution of different individual populations with different QD:Ab ratios. It is clear here that this information could be of utmost importance as the presence of a single or a mixture of bioconjugate species will surely determine the success of the subsequent application of the QDs-based nanoassembly. Successive incorporation of QDs to the final bioconjugated nanostructure leads to increased hydrodynamic size and, therefore, longer retention times in AF4. In this context, monitoring of the Cd to S intensity ratio point-by-point along the bioconjugate peak instead of the global peak area ratio could be used to assess the different individual populations likely coeluting in the broad AF4 peak. A scheme of the approach is shown in Figure 2.

Cd/S intensity ratio was then determined point-by-point for both the pure QDs and the bioconjugate peaks observed for the different bioconjugation reactions assayed (see Figures 4a-c). While the Cd/S intensity ratio profile in the peak of the pure QDs was flat and constant with an average Cd/S intensity ratio of 1.86 ± 0.02 (1SD, *n*=3), computed using 30 points in the constant central region of the peak, the Cd/S intensity ratio profile in the peak of the different bioconjugates assayed displayed a sigmoid function, as shown in Figures 4a-c. Such sigmoid curves showed two stable regions with different Cd/S intensity ratios: one plateau with a low constant Cd/S intensity ratio at the beginning of the bioconjugate peak and another one with a higher constant Cd/S intensity ratio at the end. This finding allowed us to assess individual limit populations as we assumed that within such constant regions only the bioconjugated species with

extreme QD:Ab ratios were eluting and thus the Cd/S ratio measured corresponded to them exclusively. As shown in Figure 2 we were able to characterize the lower limit (low Cd/S intensity ratio) and the upper limit (high Cd/S intensity ratio) populations. To do so we used again the Cd/S intensity ratio of the pure QDs as a reference since the Cd/S intensity ratio of the first fractographic peak corresponding to the excess of free QDs and Ab (peak at 10 min in Figures S3c-e) varied significantly for each bioconjugation reaction assayed (1.72 ± 0.05, 1.98 ± 0.03, 1.97 ± 0.04, respectively; 1SD, n=3).

Regarding data treatment, Cd and S backgrounds (average of 350 points prior to void volume peak observed at ~4.9 min) were subtracted to every intensity point of the corresponding Cd and S fractograms (see Fig. S3). Then, average Cd/S intensity ratios were computed for each constant plateau of the different bioconjugate peaks (see Table 2). In order to obtain reproducible and precise results average Cd/S intensity ratios were computed using exclusively 50 points in the constant central region of the plateau, discarding the points close to the peak front and tail. Precision obtained for the lower limit population of mixture 1:1 was worse (5% RSD) than the rest (all below 3% RSD) likely because baseline resolution of the bioconjugate peak from the excesses peak could not be fully achieved whilst it was complete for the others (see Fig. S3). In this sense, it is clear that the influence of the S background on the S measured was always more significant in the lower limit in comparison to the higher limit populations, which resulted in slightly higher uncertainties.

Next, corrected Cd/S intensity ratios computed for each limit population of the different bioconjugate peaks were translated into Cd/S molar ratios by resorting to external FI calibration (see Fig. 2). Increasing concentrations of a S inorganic standard were added to a fixed amount of a Cd inorganic standard (see Fig. S4a and S4b). In this case, Cd/S intensity ratios (peak apex) were plotted against the corresponding Cd/S molar ratios. As the number of Cd and S atoms per QDs and the number of S atoms per Ab were computed and known in advance, respectively, we could use the different Cd/S molar ratios to determine the QD:Ab ratio for each individual lower and upper limit populations within the bioconjugate peak for the different bioconjugation conditions assayed. Such individual QD:Ab ratios are also given in Table 2. Again, propagated uncertainty associated to each ratio took into account the uncertainty coming from each parameter used in the computation. As expected, the range of the QD:Ab ratios observed between lower and upper populations decreases as the excess of QDs used in the reaction

increases. QD:Ab ratio obtained for the upper limit population (1.2 ± 0.1) in the 1:1 molar ratio bioconjugation is more than four times higher than the QD:Ab ratio obtained for the lower limit population (0.27 ± 0.04). However, such difference is significantly lower, just 2.5 times (4.6 ± 0.4 and 1.8 ± 0.2, respectively) in the theoretical 3:1 molar ratio assayed.

Additionally, it is interesting to highlight the different composition of bioconjugated species detected when considering the three reactions together. In this context, the lower limit population of the 1:1 molar ratio reaction contains ~4 Ab per each QD (0.27 QD:Ab ratio) while the higher population of the 3:1 molar ratio reaction contains ~5 QD per each Ab. Again, uncertainty associated to QD:Ab ratio of the lower limit population of the 1:1 mixture assayed (15% RSD) was slightly higher because of the lack of baseline resolution mentioned before. It should be pointed out as well that a 3:1 excess of QDs per Ab in the reaction assayed is necessary to achieve both limit species populations with excess of QDs (1.8 ± 0.2 and 4.6 ± 0.4, respectively). In contrast, a 2:1 excess of QDs per Ab in the reaction assayed still led to a lower species population with a QD:Ab ratio slightly lower than 1 (0.67 ± 0.07).

At this point we are able to find out what are the two limit populations within the different bioconjugate AF4 peaks observed. We also know that the central main part of such peaks contains the mixture of unresolved bioconjugate species with intermediate QD:Ab ratios between the limit species found. Unfortunately we cannot determine the relative abundance of every individual bioconjugate species present. However, we can reduce the complexity of the system and assume that only the two found limit species are present in the peak. This made it possible to obtain their relative abundance. This information is still very interesting as it complements the finding of the limits of the range of bioconjugate species present with estimation of which are predominant in the bioconjugate mixture, either those close to the lower or upper limit. A scheme of the protocol developed to deconvolute the target bioconjugate peak is given in Figure 3. First, relative abundances of Cd and S involved in each point of the bioconjugate peak could be determined point-by-point using the intensity values obtained by ICP-MS/MS (after background correction). Thus, the Cd and S abundances in each point (A_i^{Cd} and A_i^{S}, respectively) can be expressed as the ratio between the intensity value of Cd (I_i^{Cd}) or S (I_i^{S}) and the sum of both intensity values:

$$A_i^{Cd} = \frac{I_i^{Cd}}{(I_i^{Cd} + I_i^{S})} \qquad (1)$$

$$A_i^S = \frac{I_i^S}{(I_i^{Cd} + I_i^S)} \tag{2}$$

Such Cd and S abundances obtained by eq 1 and 2 were plotted (see Figure S5a in Supporting Information) along the peak. Then, the same 50 points selected before for the average Cd/S intensity ratios were used to compute average maximum and minimum abundance values for Cd (A_{max}^{Cd} and A_{min}^{Cd}, respectively) and S (A_{max}^S and A_{min}^S, respectively). Of course, couples A_{min}^{Cd}, A_{max}^S and A_{max}^{Cd}, A_{min}^S correspond to the lower limit and upper limit populations, respectively (see Fig. 3). Relative Cd and S point-by-point intensity abundances computed before (Eqs. 1 and 2) can be then expressed as functions of the molar fractions of the lower limit QD-Ab population (χ_i^1) and the upper limit QD-Ab population (χ_i^2) and the corresponding maximum and minimum abundance values using mass balances shown in eq 3 and 4:

$$A_i^{Cd} = \chi_i^1 \cdot A_{min}^{Cd} + \chi_i^2 \cdot A_{max}^{Cd} \tag{3}$$

$$A_i^S = \chi_i^1 \cdot A_{max}^S + \chi_i^2 \cdot A_{min}^S \tag{4}$$

After rearranging eq 3 and 4, molar fraction profiles for each one of the limit populations within the bioconjugate peak (*i.e.* χ_i^1 and χ_i^2) could be obtained (see Fig. S5b). Corresponding Cd intensity values for the lower limit (Cd_i^1) and upper limit (Cd_i^2) populations could be obtained (eq 5 and 6) after multiplying point-by-point Cd intensity values (I_i^{Cd}) by the molar fractions of the individual populations obtained in each point of the peak:

$$Cd_i^1 = \chi_i^1 \cdot I_i^{Cd} \tag{5}$$

$$Cd_i^2 = \chi_i^2 \cdot I_i^{Cd} \tag{6}$$

Finally, deconvolution of the bioconjugate peak into the two limit populations could be achieved as shown in Figures 4d-f. Relative abundances of each deconvoluted population within the global bioconjugate peak were calculated by the ratio between each corresponding Cd area and the total Cd area of the original bioconjugate peak. Full set of results is collected in Table 2. It is interesting to highlight that while relative abundances of the lower and upper limit QD-Ab populations are very similar (ranged from 42 % to 58 %) when excess of QDs was assayed in the

reaction mixture, relative abundance of the lower limit population (QD:Ab ratio 0.27 ± 0.04) is very low (16 %) when using equimolar concentrations of QD and Ab. Notably, in this last particular case that higher limit population was really dominating the mixture (abundance 84 %) its QD:Ab ratio (1.2 ± 0.1) was very close to the theoretical 1:1 ratio assayed in the reaction.

Internal Validation of the Results Obtained using Both Strategies

Unfortunately, there are no certified samples available that could be used to validate our approach. This is the reason why we attempted to internally validate our qualitative and quantitative results. In this sense, taking into account the QD:Ab ratios of the two individual limit populations disclosed within the different bioconjugate peaks and their corresponding relative abundance, we could directly obtain the weighted global QD:Ab ratio for each bioconjugate mixture (peak) assayed, that corresponded to 1.1 ± 0.2, 1.9 ± 0.3 and 3.0 ± 0.4 (n=3, 1 SD). Of course final uncertainty includes individual uncertainties from the ratios and their corresponding abundances. This is the reason why increased slightly up to 13-18 % RSD. Such weighted global QD:Ab ratio could be then critically compared with the global QD:Ab ratio computed using first strategy proposed based on peak area ratio computation (see Table 1). As can be seen, QD:Ab ratios obtained using the two independent strategies match really well between them and with the theoretical QD:Ab molar ratios assayed as well.

CONCLUSIONS

Quantitative assessment of the nanoparticle:protein ratios in engineered QDs-Ab nanoassemblies mixtures has been successfully carried out. In contrast to existing methodologies, mostly based on indirect and long multi-step procedures, the herein proposed strategies rely exclusively on the metal to sulfur elemental ratios directly and accurately measured in the isolated bioconjugate peak obtained by AF4-ICP-MS/MS. The combination of the two strategies based on peak area and point-by-point intensity elemental ratios, respectively, allows in a single analysis (20 min) not only to determine the global (average) QD:Ab ratio in the nanoparticle-antibody bioconjugate mixture but also the assessment of the individual populations with extreme QD:Ab ratios within the range of species present, with additional precise estimation of their corresponding relative abundance. Of course, such abundance information is somehow limited since bioconjugate species with intermediate QD:Ab ratios are expected within the AF4 peak and

we assume that only two limit species are present. However, QD:Ab ratios computed in the limit populations provides an idea of the diversity of the bioconjugated species present in the mixture (peak) while their relative abundance informs about the importance of the corresponding populations with low and high QD:Ab ratios (beginning and end of the original peak, respectively) within such range of species. Of course, an accurate diagnosis as required in some clinical applications, would require more detailed information on the different NP:protein compositions. In this context, it is worth noting that increasing resolution of the separation by AF4 would bring about more accurate information on the composition of the different biocojugates.

The approach proposed is general and could be applied to any type of inorganic NP containing sulfur, either in the core (*e.g.* ZnS), shell (*e.g.* CdSe/CdS) or the ligands attached to their surface (*e.g.* Au or Ag NPs surrounded by cysteine or DHLA), and functionalized by bioconjugation to sulfur-containing biomolecules, especially proteins (*e.g.* antibodies, avidin). Of course, the only requisite to meet is that the conjugation of the S-containing biomolecules to the NP must result in a change in the S to Cd ratio that could be measured by ICP-MS/MS. Interestingly, the absence of sulfur in the NP under study (i.e. Au or Ag surrounded by citrate or Si-based) would facilitate enormously the approach making it more accurate and precise since the only S source would be the biomolecule in this case. It would be the same if the biomolecule would contain an ICP-MS detectable element different than S. Additionally our approach is not constrained by the type of NP-biomolecule interaction, no matter if chemical (bioconjugation) or mostly physical (protein corona).

A profound impact in many scientific disciplines is expected. In this sense, it can be clearly envisaged its application as diagnostic tool for the assessment of the different complex nanoassemblies used in NP-based immunoassays (clinical), imaging and trafficking studies or drug delivery. There is an urgent need of quality control tools in the production of such fit-for-purpose engineered nanoassemblies.[4] Notably, once different populations are identified in bioconjugated peaks, fractions can be collected to obtain conjugate solutions with targeted and mostly single QD:Ab ratios.

ASSOCIATED CONTENT
Supporting Information

AUTHOR INFORMATION

Corresponding Authors

*E-mail: *jcostafe@uniovi.es*

*E-mail: *ruizjorge@uniovi.es*

Notes

The authors declare no competing financial interest.

ACKNOWLEDGMENTS

REFERENCES

(1) Mattoussi, H.; Palui, G.; Bin Na, H. Luminescent quantum dots as platforms for probing in vitro and in vivo biological processes. *Adv. Drug Deliv. Rev.* **2012**, 64, 138-166.

(2) Karakoti, A. S.; Shukla, R.; Shanker, R.; Singh, S. Surface functionalization of quantum dots for biological applications. *Adv. Colloid Interface Sci.* **2015**, *215*, 28-45.

(3) Montenegro, J.-M.; Grazu, V.; Sukhanova, A.; Agarwal, S.; de la Fuente, J. M.; Nabiev, I.; Greiner, A.; Parak, W. J. Controlled antibody/(bio-) conjugation of inorganic nanoparticles for targeted delivery. *Adv. Drug Deliv. Rev.* **2013**, 65, 677-688.

(4) del Pino, P.; Pelaz, B.; Zhang, Q.; Maffre, P.; Ulrich Nienhaus, G.; Parak, W. J. Protein corona formation around nanoparticles – from the past to the future. *Mater. Horiz.* **2014**, 1, 301-313.

(5) Jiang, X.; Jiang, J.; Jin, Y.; Wang, E.; Dong, S. Effect of colloidal gold size on the conformational changes of adsorbed cytochrome c: Probing by circular dichroism, UV-visible, and infrared spectroscopy. *Biomacromolecules* **2005**, *6*, 46-53.

(6) Wu, X.; Narsimhan, G. Characterization of secondary and tertiary conformational changes of β-Lactoglobulin adsorbed on silica nanoparticle surfaces. *Langmuir* **2008**, *24*, 4989-4998.

(7) Claridge, S. A.; Liang, H. W.; Basu, R. B.; Frechet, J. M. J.; Alivisatos, A. P. Isolation of discrete nanoparticle-DNA conjugates for plasmonic applications. *Nano Lett.* **2008**, *8*, 1202-1206.

(8) Song, F.; Chan, W. C. W. Principles of conjugating quantum dots to proteins via carbodiimide chemistry. *Nanotechnology* **2011**, *22*, 494006-494012.

(9) Sapsford, K. E.; Tyner, K. M.; Dair, B. J.; Deschamps, J. R.; Medintz, I. L. Analyzing nanomaterial bioconjugates: A review of current and emerging purification and characterization techniques. *Anal. Chem.* **2011**, *83*, 4453–4488.

(10) Liu, S.; Horak, J.; Höldrich, M.; Lümmerhofer, M. Accurate and reliable quantification of the protein surface coverage on protein-functionalized nanoparticles. *Anal. Chim. Acta* **2017**, *989*, 29–37.

(11) Hinterwirth, H.; Kappel, S.; Waitz, T.; Prohaska, T.; Lindner, W.; Lammerhofer, M. Quantifying thiol ligand density of self-assembled monolayers on gold nanoparticles by inductively coupled plasma-mass spectrometry. *ACS Nano* **2013**, *7*, 1129-1136.

(12) Bouzas-Ramos, D.; Menendez-Miranda, M.; Costa-Fernandez, J. M.; Ruiz Encinar, J.; Sanz-Medel, A. Precise determination of the nanoparticle concentration and ligand density of engineered water-soluble HgSe fluorescent nanoparticles. *RSC Adv.* **2016**, *6*, 19964-19972.

(13) Garcia-Cortes, M.; Sotelo Gonzalez, E.; Fernández-Arguelles, M. T.; Ruiz Encinar, J.; Costa-Fernandez, J. M.; Sanz-Medel, A. Capping of Mn-doped ZnS quantum dots with DHLA for their stabilization in aqueous media: Determination of the nanoparticle number concentration and surface ligand density. *Langmuir* **2017**, *33*, 6333−6341.

(14) Fernandez-Iglesias, N.; Bettmer, J. Complementary mass spectrometric techniques for the quantification of the protein corona: A case study on gold nanoparticles and human serum proteins. *Nanoscale* **2015**, *7*, 14324-14331.

(15)   Matczuk, M.; Legat, J.; Shtykov, S. N.; Jarosz, M.; Timerbaev, A. R. Characterization of the protein corona of gold nanoparticles by an advanced treatment of CE-ICP-MS data. *Electrophoresis* **2016**, *37*, 2257–2259.

(16)   Bouzas-Ramos, D.; Garcia-Cortes, M.; Sanz-Medel, A.; Ruiz Encinar, J.; Costa-Fernández, J. M. Assessment of the removal of side nanoparticulated populations generated during one-pot synthesis by asymmetric flow field-flow fractionation coupled to elemental mass spectrometry. *J. Chromatogr. A* **2017**, *1519*, 156–161.

(17) Menendez-Miranda, M.; Presa-Soto, D.; Presa-Soto, A.; Costa-Fernandez, J.M.; Ruiz Encinar, J. Isotopically enriched nanoparticles in combination with mass spectrometry for the assessment of nanoparticle-biomolecule stoichiometries in engineered nanoassemblies. *Spectrochim. Acta B* **2018**, *149*, 99-106.

(18)   Calderón-Celis, F.; Diez-Fernández, S.; Costa-Fernández, J. M.; Ruiz Encinar, J.; Calvete, J. J.; Sanz-Medel, A. Elemental mass spectrometry for absolute intact protein quantification without protein-specific standards: Application to snake venomics. *Anal. Chem.* **2016**, *88*, 9699-9706.

(19)   Calderón-Celis, F.; Sanz-Medel, A.; Ruiz Encinar, J. Universal absolute quantification of biomolecules using element mass spectrometry and generic standards *Chem. Commun.* **2018**, *54*, 904-907.

(20)   Peng, Z. A.; Peng, X. Formation of high-quality CdTe, CdSe, and CdS nanocrystals using CdO as precursor. *J. Am. Chem. Soc.* **2001**, *123*, 183-184.

(21)   Pellegrino, T.; Manna, L.; Kudera, S.; Liedl, T.; Koktysh, D.; Rogach, A. L.; Keller, S.; Radler, J.; Natile, G.; Parak, W. J. Hydrophobic nanocrystals coated with an amphiphilic polymer shell: A general route to water soluble nanocrystals. *Nano Lett.* **2004**, *4*, 703-707.

(22)   Fernandez-Arguelles, M. T.; Yakovlev, A.; Sperling, R. A.; Luccardini, C.; Gaillard, S.; Sanz-Medel, A.; Mallet, J. M.; Brochon, J. C.; Feltz, A.; Oheim, M.; Parak, W. J. Synthesis and characterization of polymer-coated quantum dots with integrated acceptor dyes as FRET-based nanoprobes. *Nano Lett.* **2007**, *7*, 2613-2617.

(23)   Menendez-Miranda, M.; Ruiz Encinar, J.; Costa-Fernandez, J. M.; Sanz-Medel, A. Asymmetric flow field-flow fractionation coupled to inductively coupled plasma mass spectrometry for the quantification of quantum dots bioconjugation efficiency. *J. Chromatogr. A* **2015**, *1422*, 247-252.

(24)   Yu, W. W.; Qu, L.; Guo, W.; Peng, X. Experimental determination of the extinction coefficient of CdTe, CdSe, and CdS nanocrystals. *Chem. Mater.* **2003**, *15*, 2854-2860.

(25)   Arruebo, M.; Valladares, M.; González-Fernández, A. Antibody-conjugated nanoparticles for biomedical applications. *J. Nanomater.* **2009**, *439389*, 1-24.
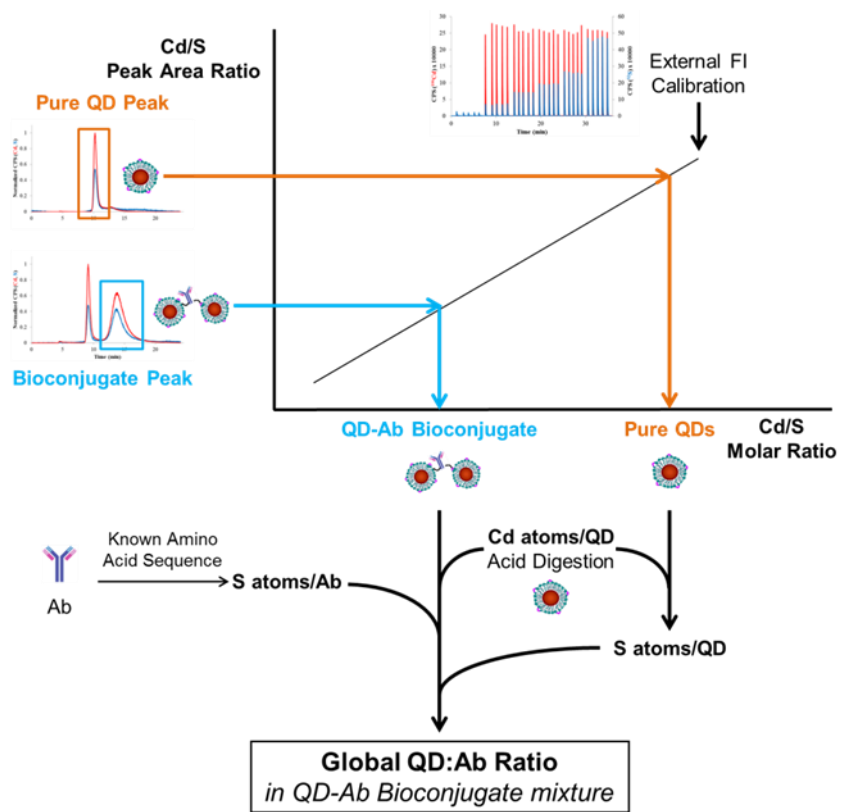
Figure 1. Workflow employed for the determination of the global (average) QD:Ab ratio in the different bioconjugate mixtures assayed using peak area ratio computation.
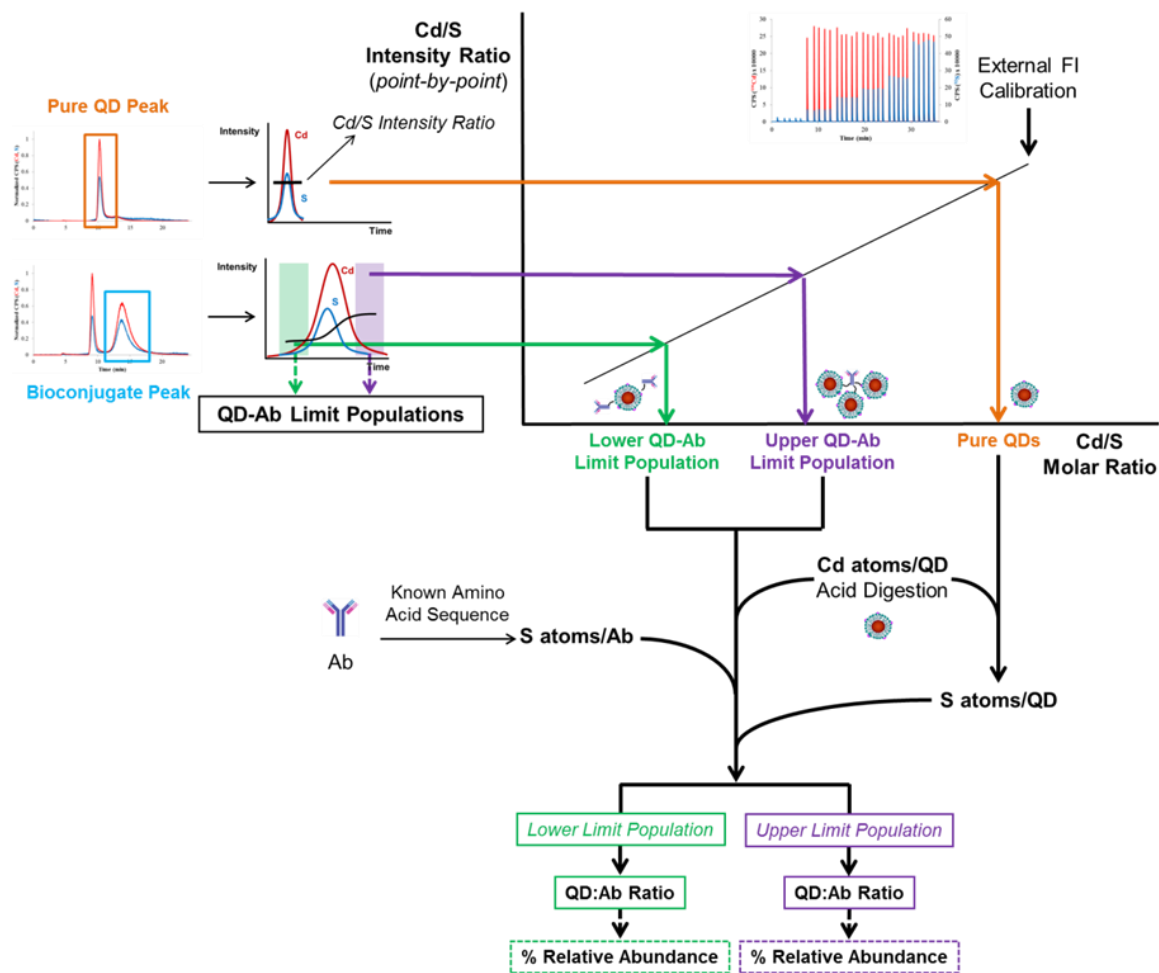
Figure 2. Workflow employed for disclosing the mixture of individual populations with different QD:Ab ratio in the different bioconjugate mixtures assayed using point-by-point intensity ratio computation.
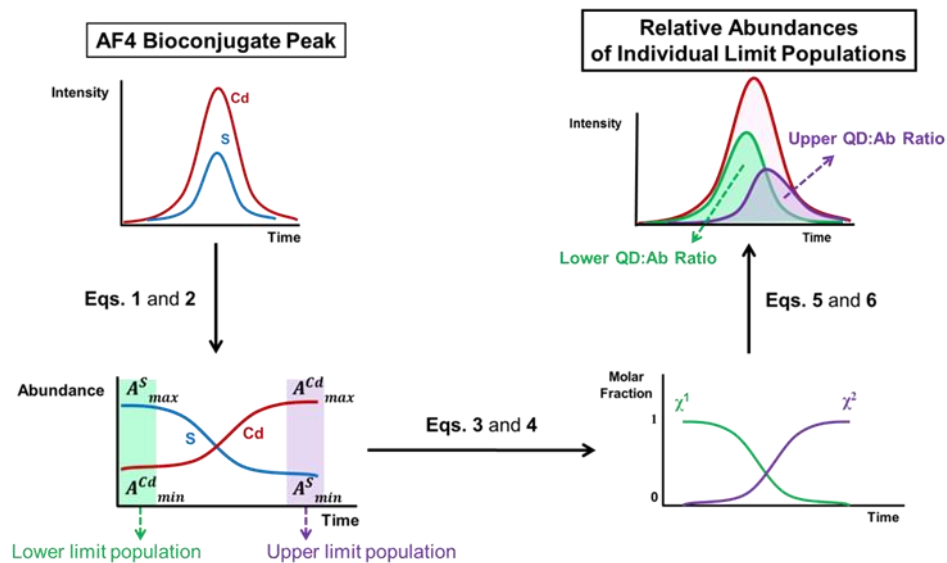
Figure 3. Workflow employed for the deconvolution and determination in the bioconjugate peak of relative abundances of individual limit populations
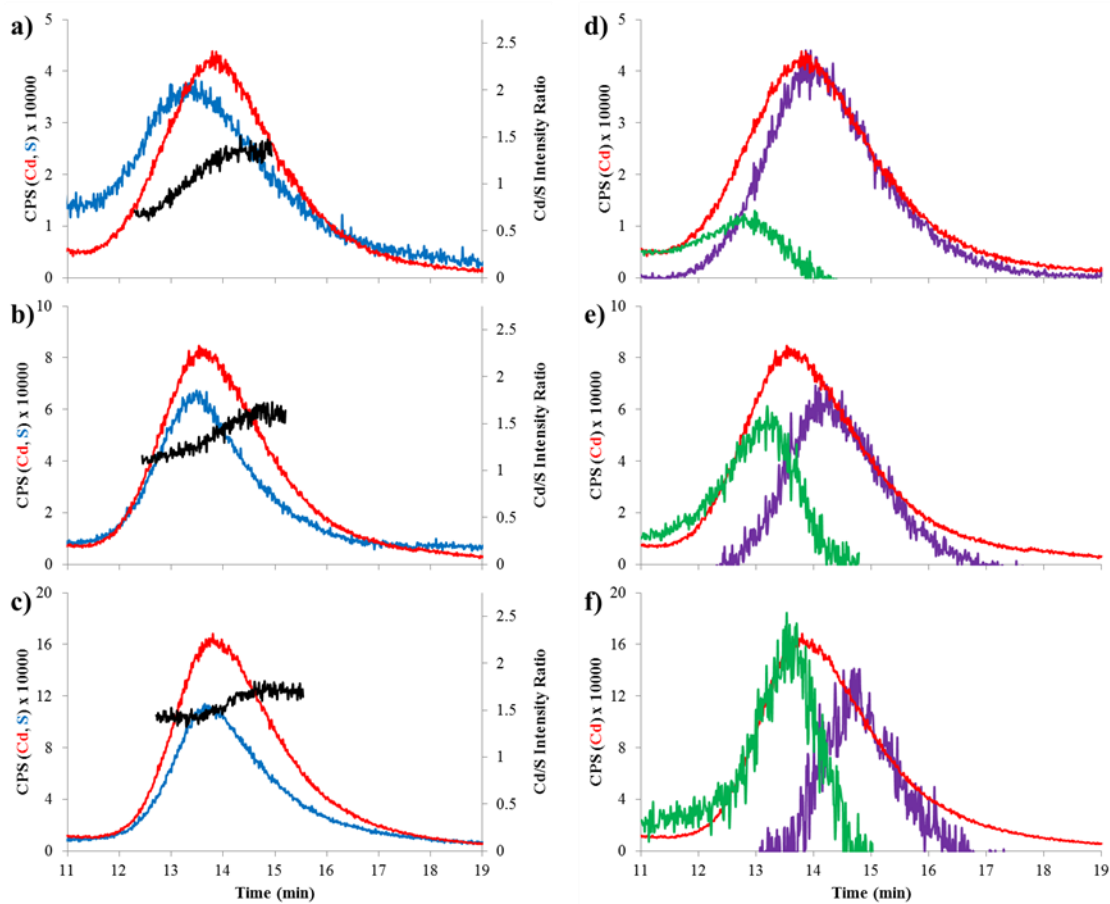
Figure 4. a-c) ICP-MS/MS fractograms of the bioconjugate peak and d-f) deconvolution into the two limit populations obtained for the different bioconjugation mixtures QD-Ab assayed: a,d) 1:1; b,e) 2:1; c,f) 3:1. Red line: ^{106}Cd bioconjugate peak; blue line: ^{32}S bioconjugate peak; black line: Cd/S intensity ratio profile in the bioconjugate peak; green line: lower limit population; purple line: upper limit population.

Table 1. Bioconjugation efficiencies, area ratios and global (average) QD:Ab ratios obtained in the bioconjugation peak for the different mixtures assayed (n=3, propagated uncertainty corresponds to 1SD).

Molar Ratio QD:Ab Assayed	Bioconj. Efficiency (%)	Cd/Se Area Ratio	Cd/S Area Ratio	Molar Ratio QD:Ab obtained
1:1	60 ± 2	1.72 ± 0.04	1.27 ± 0.03	**1.2 ± 0.1**
2:1	68 ± 3	1.72 ± 0.03	1.46 ± 0.03	**2.1 ± 0.2**
3:1	74 ± 2	1.71 ± 0.06	1.57 ± 0.02	**3.2 ± 0.3**

Table 2. Cd/S intensity ratios, QD:Ab ratios and relative abundances of the individual lower and upper limit populations within the bioconjugate peak and weighted QD:Ab ratios obtained for the different bioconjugation reactions assayed ($n=3$, propagated uncertainty corresponds to 1SD).

Molar Ratio QD:Ab Assayed	Cd/S Intensity Ratio	Molar Ratio QD:Ab obtained	Relative Abundance (%)
Lower Limit Population			
1:1	0.66 ± 0.03	0.27 ± 0.04	16 ± 1
2:1	1.07 ± 0.03	0.67 ± 0.07	42 ± 2
3:1	1.46 ± 0.03	1.8 ± 0.2	55 ± 2
Upper Limit Population			
1:1	1.33 ± 0.02	1.2 ± 0.1	84 ± 2
2:1	1.58 ± 0.02	2.8 ± 0.3	58 ± 2
3:1	1.67 ± 0.02	4.6 ± 0.4	45 ± 2

For TOC only